Elongation of Fibers from Highly Viscous Dextran Solutions Enables Fabrication of Rapidly Dissolving Drug Carrying Fabrics

*John P. Frampton, David Lai, Maxwell Lounds, Kyeongwoon Chung, Jinsang Kim, John F. Mansfield, and Shuichi Takayama**

A simple method is presented for forming thread-like fibers from highly viscous dextran solutions. Based on the cohesive and adhesive forces between a dextran solution and the substrate to which it is applied, multiple fibers of approximately 10 µm in diameter can be elongated simultaneously. These fibers can be woven into multiple layers to produce fabrics of varying fiber orientations and mechanical properties. Various bioactive agents can be incorporated into the dextran solution prior to fiber formation, including hemostatic and antibiotic agents. Fabrics containing thrombin are capable of coagulating human platelet poor plasma in vitro. Fabrics containing antibiotics are capable of suppressing bacterial growth in a disk diffusion assay. These data suggest that this new material composed entirely of dextran has promise as a drug delivery component in wound dressings.

1. Introduction

Topical, transdermal, and oral treatment systems often involve the release of bioactive compounds from a delivery matrix.[1–5] In the case of topical or transdermal treatment systems, the delivery matrix often takes the form of a thin, planar material that is brought into conformal contact with the skin or the mucosal tissue. These systems are often fabricated using electrospun polymeric scaffolds that allow the rate of drug release to be controlled by tuning the pore size and interconnectivity of the scaffold, among other factors.[3,6] Similar types of scaffolds have been applied as wound dressings.[3,7,8] To facilitate healing and control drug release rates, the latest scaffolds are often biodegradable with tunable biodegradation rates.

There are also several other types of topical wound dressings available for the treatment of open wounds such as lacerations, abrasions, and burns.[1,5,9] Many of these wound dressings incorporate biopolymers, such as collagen and fibrin, to promote wound healing or reduce scarring.[8,10–15] For example, collagen- and fibrin-based materials have been applied to wounds by implantation or injection in combination with other surgical procedures. It is also possible to apply biopolymer scaffolds in the form of sponge-type constructs. For example, chitosan and collagen sponges have been used as topically applied wound dressings for burns and abrasions to promote wound healing.[10,15] These materials also provide the ability to release factors that can promote bioresorption and tissue remodeling at the wound site.

In addition to their applications as wound dressing materials, polymer-based fiber materials, which can be fabricated through electrospinning, have found applications as filtration matrices, coating films, drug release scaffolds, and tissue engineering materials.[16,17] Electrospinning can be used to produce biopolymer matrices composed of fibers ranging in diameter from tens of nanometers to several micrometers that can potentially carry drugs or promote remodeling of injured tissues by serving as a matrix for cell interaction.[7,16,18–21] Importantly, as mentioned above, these electrospun materials can be tuned to provide optimal fiber sizes, pore sizes, and fiber orientations for specific applications.[16] Moreover, the high surface area of the fiber architecture can enhance drug release and bioresorption.[22]

There are, however, several drawbacks to electrospun fabrics, including the time and equipment required for their fabrication, which have limited their widespread adoption by the scientific community. Electrospinning also at times suffers from fabrication defects in the form of beading[23] and pores[24] within the polymer fibers. Moreover, the types of polymers that can be electrospun are sometimes limited because the nozzles used for liquid jetting can become clogged by viscous polymer solutions. To overcome limitations in beading and to adjust the viscosity to control the range of fiber diameters, filler materials are typically incorporated into the polymer solutions prior to electrospinning.[25,26] However, this presents an additional problem in that the filler material may interfere with downstream biomedical applications, either by remaining in trace amounts in the final material or by interfering with the bioactivity of the drug or protein components incorporated into the polymeric material.

Here, we present a simple and rapid method for forming microscale diameter polymer fibers without the use of electrospinning. This method can be used to form dextran fabrics capable of carrying and delivering drugs such as hemostatic

J. P. Frampton, D. Lai, M. Lounds, K. Chung, J. Kim, J. F. Mansfield, Prof. S. Takayama
University of Michigan, Biointerfaces Institute
Ann Arbor, MI 48108, USA
E-mail: takayama@umich.edu

DOI: 10.1002/adhm.201400287

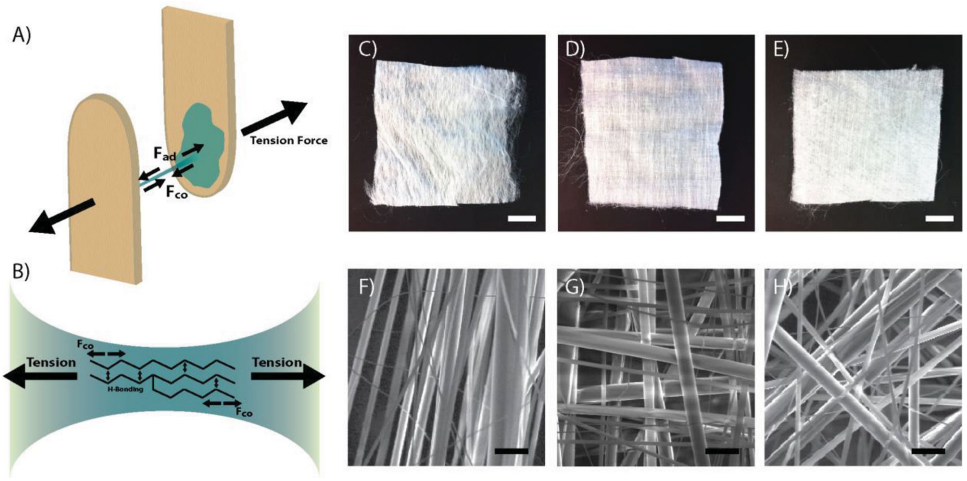

Figure 1. Formation of dextran fibers by elongation and drying of liquid strings of dextran solution. A) Highly viscous solutions of dextran form liquid strings between two substrates due to adhesive forces (F_{ad}) between the dextran solution and the substrate and cohesive forces (F_{co}) within the dextran solution as the solution is pressed between two substrates that are then moved apart to generate tension. B) On the molecular level, the cohesive forces are derived from entanglement of the dextran polymer chains and interchain hydrogen bonding. C–E) Multiple fibers can be elongated simultaneously to produced multilayered fabrics with the fibers oriented in one direction (180° symmetry; C), two directions (90° symmetry; D) and multiple directions (45° symmetry; E). Scale bars are 10 mm. F–H) SEM images of the fabrics with fibers oriented in one direction (F), two directions (G), and multiple directions (H). Scale bars are 50 μm.

agents and antibiotics. This method takes advantage of the adhesive/cohesive forces of highly viscous dextran solutions stretched between two substrates, resulting in the formation of fibers that rapidly dry in air due to their high surface area without the use of any solvents other than water. The material properties of these fabrics are characterized by mechanical failure testing and scanning electron microscopy (SEM). We demonstrate a medical application for these dextran fabrics by delivering thrombin and antibiotics by way of rapid dissolution of the dried fabrics upon contact with moist surfaces. The dextran fabrics are capable of clotting human platelet poor plasma and preventing bacterial growth on agar plates. Since medical grade (FDA approved) dextran is already commercially available and lends itself to medical applications, these proof-of-concept experiments may lead to further applications of dextran fabrics as topical or oral drug delivery systems or as advanced wound healing/remodeling materials.

2. Results

2.1. Dextran Fabric Generation and Characterization

The 500 000 g mol^{-1} dextran used in this study was soluble in water up to a concentration of approximately 60 wt% (Figure S1, Supporting Information). At 70 wt% the dextran formed an opaque nearly-solid material. At concentrations above 70 wt% there were significant quantities of dry dextran that were not incorporated into the mixture. Concentrations of dextran between 40 and 60 wt% were capable of forming fibers by tension between two substrates. As strands of dextran solution extended from the dextran source, evaporative water loss occurred, resulting in dry fibers with diameters of approximately 10 μm, which varied depending on the concentration of the dextran source solution and the strain rate of fiber extension. It was possible to form multiple fibers simultaneously by increasing the cross-sectional area of the dextran volume under tension between two relatively large, flat substrates, such as wooden tongue depressors, that were brought into conformal contact before extending them apart with a swift motion.

When the dextran solution is in contact with the substrates (in this case the wooden tongue depressors), many of the dextran chains will be coiled and entangled among each other. The polymer solution elongates from a number of contact points between the two substrates. As the tongue depressors are separated, tensile stress is imposed on the dextran chains as the highly viscous dextran solution dries, likely resulting in uncoiling and elongation of the dextran chains. Adhesive forces keep the dextran solution attached to each wooden tongue depressor, while cohesive forces between the dextran chains prevent the strands of dextran solution from breaking (**Figure 1**A). The strands of dextran solution are able to withstand significant elongation forces (generated manually) without breaking because of the cohesive forces in the solution and the hydrogen bonding between the chains and branches of the dextran molecules (Figure 1B).[27,28] This combination of the adhesive and cohesive forces in the system allows strands of dextran solution to be formed that dry rapidly in air to form dextran fibers.

A total of nine types of fabrics were generated by this fiber extension process, including fabrics of three different thicknesses (generated by 50, 100, or 200 layered fiber extensions) with three different orientations (unidirectional, bidirectional, or multidirectional by rotating the fabric between extensions). Macroscopic and SEM images of the fabrics are shown in Figure 1C–H. These fabrics were submitted to mechanical uniaxial tensile testing with the direction of strain aligned with, perpendicular to or at a 45° to the main orientation of the dextran fibers in the fabrics (**Figure 2**A–C). The toughness of the fabric decreased with the number of fiber layers for all of the fabric types, as indicated by the force displacement curves

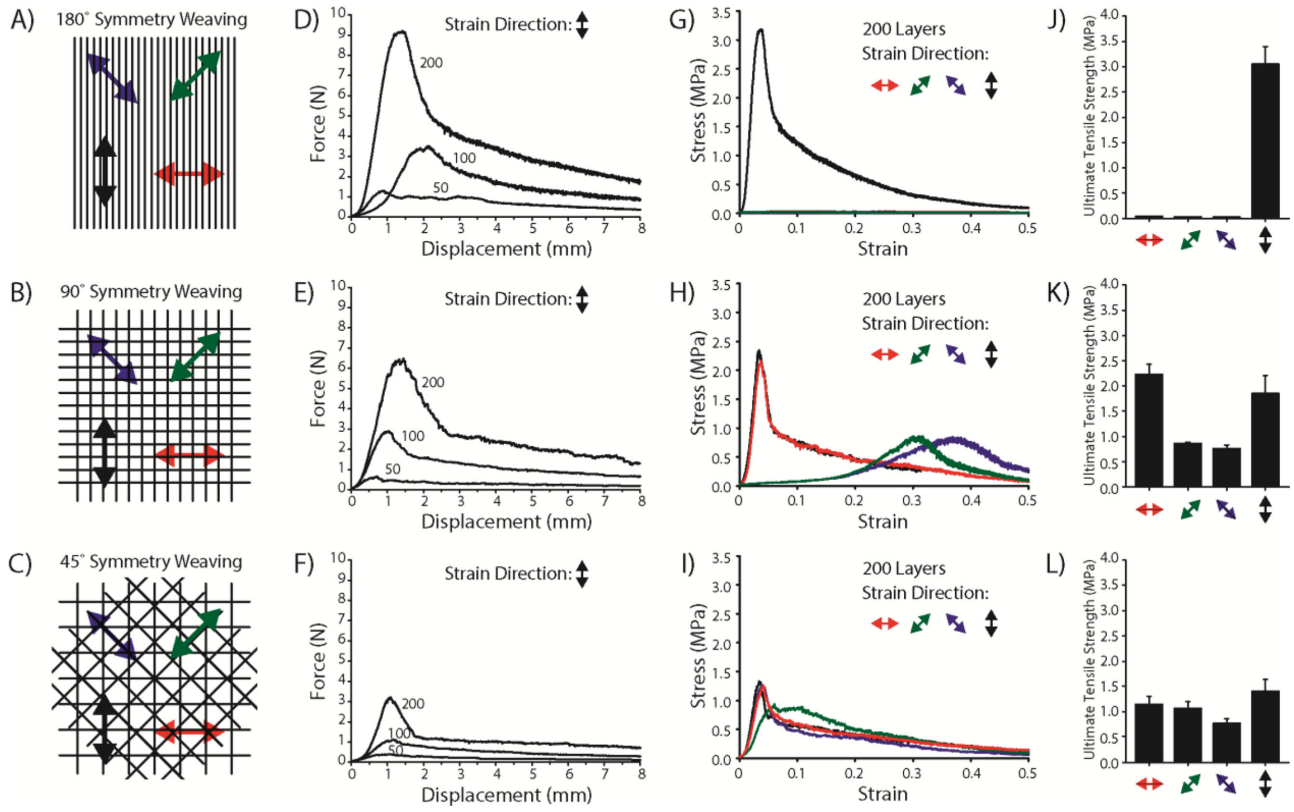

Figure 2. Mechanical testing of the dextran fabrics. A–C) Schematic representations of the fiber orientations with the relative directions of strain indicated by the colored arrows for the unidirectional fabrics (180° symmetry; A), bidirectional fabrics (90° symmetry; B) and multidirectional fabrics (45° symmetry; C). D–F) Force-displacement data in the vertical direction of strain for the unidirectional fabrics (D), bidirectional fabrics (E), and multidirectional fabrics (F) for 50, 100, and 200 layers of fibers. G–I) Stress-strain data for all four directions of strain for the unidirectional (G), bidirectional (H), and multidirectional (I) fabrics for 200 layers of fibers. J–L) The corresponding ultimate tensile strength data obtained from plots (G–I).

(Figure 2D–F). Fabrics with a greater number of fibers aligned with the direction of strain were able to endure greater loads for the same number of dextran fiber layers. As expected, the unidirectional (180° symmetry) fabrics were able to withstand strain only when the direction of strain was aligned with the fibers (Figure 2G). This fabric type also had the greatest ultimate tensile strength in a single direction. The mechanical properties of the bidirectional (90° symmetry) fabrics were the same in the horizontal and vertical strain directions, but were slightly weaker when strain was applied diagonal to the fiber orientation (Figure 2H). The mechanical properties of the multidirectional (45° symmetry) fabrics were the same for each strain direction (Figure 2I). These tendencies are apparent from the stress strain curves (Figure 2G–I) and ultimate tensile strength graphs (Figure 2J–L). The mechanical testing indicates that the fabrics have sufficient strength for manufacturing and handling during medical procedures. Moreover, the fiber orientation can be used to design fabrics that are strong in one direction, but can be easily torn in another direction.

2.1. Drug Delivery using Dextran Fabrics

We tested the fabrics as vehicles for drug delivery by delivering thrombin and antibiotics in vitro. SEM analysis revealed that there was no difference in fiber diameter when thrombin was incorporated into the fibers (Figure S2, Supporting Information). We used a microplate assay based on absorbance at 405 nm to examine the kinetics of thrombin-induced plasma coagulation. When thrombin solution was added directly to the plasma, we observed a dose-dependent increase in the absorption at 405 nm due to polymerization of the fibrinogen in the plasma into fibrin (Figure S3, Supporting Information). Based on this calibration data, we selected a thrombin concentration of 31 U mL^{-1} for subsequent experiments. For comparison of the microplate absorbance data between the four thrombin conditions, 1) plasma -thrombin, 2) plasma +thrombin, 3) plasma +dextran fabric only, and 4) plasma +dextran fabric containing thrombin, the values were normalized.

The plasma only condition displayed a low baseline that fluctuated around 0.4, whereas when the thrombin solution was added, a rapid increase to maximum was observed over the course of approximately 10 min (**Figure 3**A). When the dextran fabrics were applied to the plasma, we observed a sharp increase in the absorbance due to the fabric alone, which gradually decreased over the course of the data collection period (Figure 3B, black symbols). This was likely due to the colloidal dissolution of the dextran fabric interfering with the optical measurements. When thrombin-containing fabrics were applied to the plasma, the absorbance rapidly increased in the

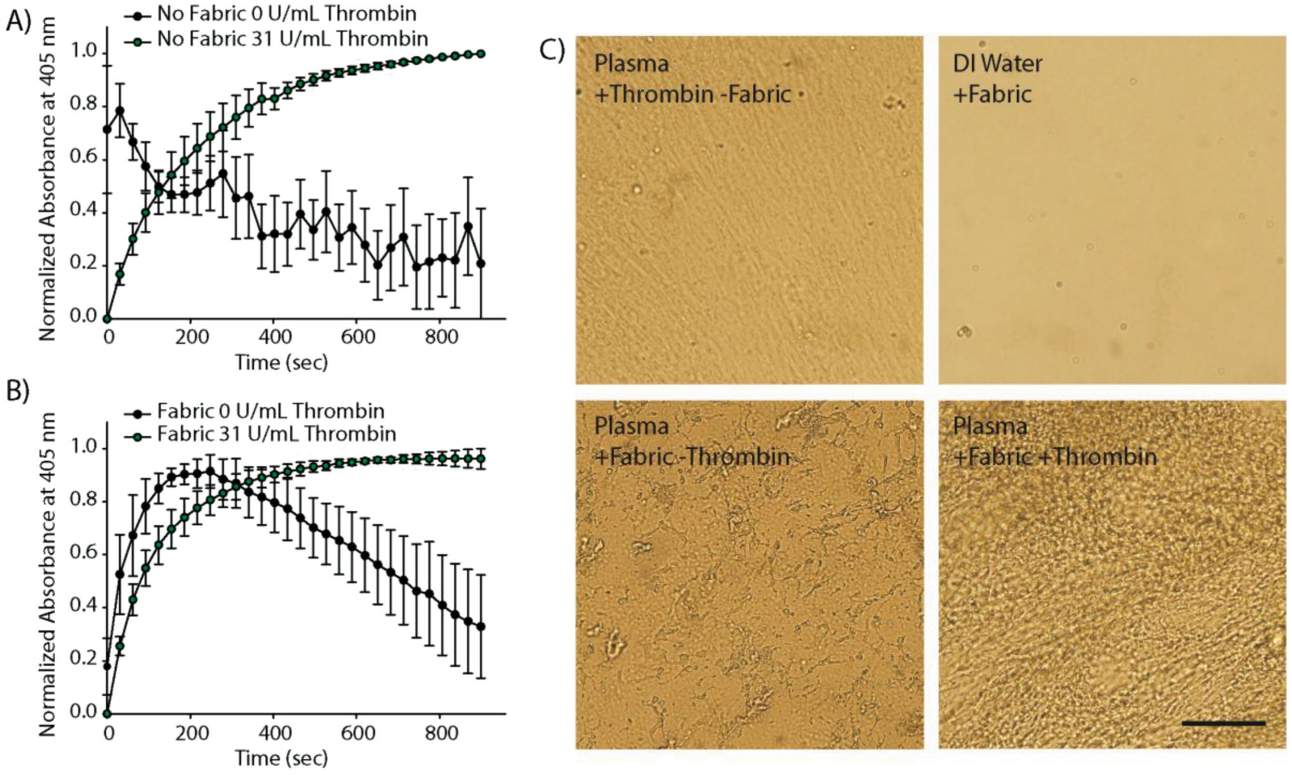

Figure 3. Dextran fabrics containing thrombin are capable of clotting plasma in vitro. A) Normalized absorbance at 405 nm for control plasma (No Fabric/0 U mL^{-1} Thrombin; black symbols) and plasma with thrombin added in solution (No Fabric/ 31 U mL^{-1} Thrombin; green symbols). The absorbance at 405 nm increases to its maximum by ≈500 s with thrombin. B) Normalized absorbance at 405 nm for plasma with the dextran fabric alone (black symbols) and with the dextran fabric containing thrombin (green symbols). The fabric alone interferes with the absorbance measurement at early time points in the assay. The absorbance at 405 nm increases to its maximum by ≈500 s with the addition of thrombin, similar to when thrombin is added to plasma without the fabric. C) Optical microscopy with a linear polarizing filter revealed that the artifact present in the absorbance data was likely caused by incomplete colloidal dispersion of the dextran fabric in the plasma (bottom left). The plasma coagulated with the fabric containing thrombin displayed microscopic structures that were qualitatively similar to those observed when the plasma was coagulated with thrombin alone. Scale bar is 50 μm.

first 10 min, after which time the absorbance stabilized, similar to when thrombin solution was added directly to the plasma (Figure 3B, green symbols).

These data were corroborated by microscopic observation of fibrin polymerization (Figure 3C). The plasma to which the thrombin solution was added directly displayed microscopic structures that we ascribed to fibrin polymerization. These structures were absent when only water was added to the plasma. We observed incomplete colloidal dispersion of the dextran (without thrombin) after it was added to the plasma. The fabric alone was not capable of coagulating the plasma based on our observation of the absence of plasma gelation. Finally, when thrombin was delivered using the fabric as a vehicle, microscopic structures similar to those observed for thrombin added in solution were observed. We confirmed plasma coagulation after imaging by manually manipulating the fabric-treated clots. We also tested the ability to deliver antibiotics using a disk diffusion assay with BL21 *Escherichia coli* (**Figure 4**). The dextran fabrics dissolved immediately upon contact with the agar plate. The fabrics alone were not capable of suppressing bacterial growth. However, we observed increased areas of clearance with increasing concentrations of antibacterial agents in the fabrics.

3. Discussion

Examples of advanced wound dressing systems range from fibrin and collagen glues to biomaterial sponges and electrospun polymer composites, all of which can be designed to stop bleeding, promote tissue remodeling, and deliver drugs or factors to aid in tissue repair or prevent infection. There are several examples of dextran-based materials fabricated by electrospinning.[7,18–20,29–32] These materials are typically polymer blends, for example, dextran/PLGA, that range in fiber diameter from hundreds of nanometers to tens of micrometers.[7,29] Electrospun dextran materials are typically cross-linked to limit their solubility, although most are bioresorbable. In this report, we produced dextran fabrics that were qualitatively similar to the electrospun dextran mats reported in previous studies. However, unlike the previous examples of cross-linked dextran fibers, our fibers were not cross-linked, allowing them to rapidly dissolve upon contact with moist surfaces. Although our fabric materials do not currently utilize polymer blends or cross-linking methods to stabilize the fibers, these approaches could be implemented to provide additional functionality.

It is worth noting that almost all of the previous studies on dextran fiber mats/fabrics used electrospinning as a fabrication

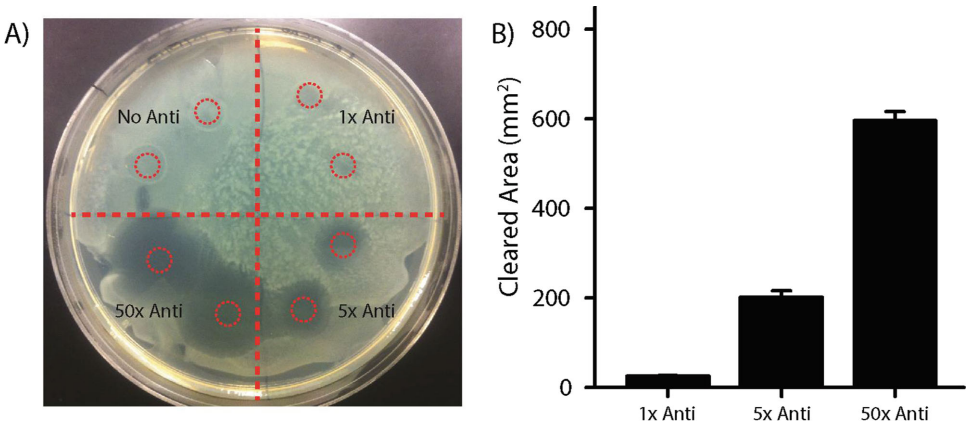

Figure 4. Antibiotics incorporated into dextran fabrics suppress bacterial growth in a disk diffusion assay. Anti–anti (penicillin, streptomycin and fungizone) was incorporated into the 50% dextran solution prior to fiber/fabric formation. A) Biopsy punches (6 mm in diameter containing different concentrations of anti–anti) were placed on LB agar plates freshly seeded with *E. coli* BL21 cells. The fabrics dissolve upon contact with the moist agar surface, releasing the antibiotics. The red dashed circles indicate the approximate coverage area of the biopsy punches. B) Quantification of the disk diffusion assay for $n = 3$ agar plates. The actual quantities of anti–anti delivered to the surface of the plates were 1× (0.06 U penicillin, 0.06 mg streptomycin and 0.16 ng fungizone), 5× (0.31 U penicillin, 0.31 mg streptomycin, and 0.78 ng fungizone), and 50× (3.1 U penicillin, 3.1 mg streptomycin and 7.75 ng fungizone).

method. Electrospinning has its roots in more traditional fiber spinning techniques,[33] such as dry spinning,[34,35] which is similar to our method, wet spinning,[36] and other industrial spinning methods including extrusion spinning and melt spinning. Electrospinning offers the advantage that it can be used to generate ultrafine nanoscale fibers with directed orientations. These fibers can be collected on a variety of substrates of various sizes and geometries.[37] However, since electrospinning requires a substrate, electrospun materials are typically used as thin coatings. Although our fibers are larger in diameter than those typically achieved by electrospinning, we are also able to orient the fibers in multiple direction, while offering the advantage of having a free standing fabric material, rather than a fabric-like mat coated on a larger solid substrate.

In many cases, cross-linked electrospun mats are used for drug delivery, but the drugs are typically added after spinning to avoid exposure to solvent, or harsh drying or cross-linking conditions. Our method for generating fabrics does not involve the use of any organic solvents, allowing sensitive drugs or proteins to be directly incorporated into the fibers. In contrast, if drugs or proteins are directly incorporated into electrospun polymers, they may become damaged or denatured by exposure to organic solvents or other factors that are commonly used to promote more consistent jetting from the electrospinning head and reduce the fiber diameter. Since dextran is also used as an excipient and a stabilizer for drugs and proteins, it may also help to maintain the activity of the reagents incorporated in the fibers.

As described above, materials similar to our dextran fabrics have found a variety of biomedical application ranging from drug delivery to wound dressings. Similar materials have been tested for BSA and lysozyme delivery in vitro,[30] VEGF delivery to HUVECs in vitro[18] and antibacterial agent delivery.[7] These materials have also found applications as cell scaffolds for fibroblasts and other cell types.[19–21] Their high surface areas, ability to release active biomolecules, biocompatibility, and ability to serve as a matrix for cells makes them ideal materials for wound dressings. In our study, we used fabrics entirely composed of non-cross-linked dextran to deliver hemostatic agents and antibiotics. Our fabrics dissolved immediately upon contact with moist surfaces, releasing their bioactive constituents. This offers the possibility of immediate release as a component of a multicomponent wound dressing with other cross-linked or slowly degrading components. It might also be possible to use this fiber forming method to form fabrics from other polymers with biomedical applications (e.g., carbohydrate polymers such as alginate, chitosan, or cellulose derivatives).

One caveat of this system is that dextran is known to interfere with coagulation.[38–41] This effect seems to be mediated through hemodilution along with non-specific interference with the coagulation system. These effects are more pronounced with lower molecular weight dextrans, especially when applied in large volumes to the blood, and may result from interference caused by colloidal interactions. In our system, we observed interference of dextran with the coagulation assay. We hypothesized that this was partially caused by incomplete dissolution of the dextran in the plasma. This was confirmed by the polarized microscopy images that showed dextran aggregates in the plasma. Interestingly, the presence of high molecular weight (500 000 g mol^{-1}) dextran did not seem to interfere with thrombin-catalyzed fibrin polymerization, as indicated by the absorbance data, the morphology of the clotted plasma and our observation that gel-like clots formed after thrombin delivery by way of the dextran fabrics. However, more detailed testing beyond the scope of this proof-of-concept study will be required to conclusively demonstrate a lack of interference with clotting or wound healing when thrombin is applied with dextran. Similar colloidal/insolubility effects were not observed in buffers, water, or on the surface of the agar plates used in the disk diffusion assay for antibiotic delivery testing.

4. Conclusions

We developed a new fabric material composed of microscale dextran fibers that can be easily fabricated without complex equipment. We applied this new fabric material for delivery of bioactive reagents such as hemostatic drugs and antibiotics. We characterized the mechanical properties of fabrics with different fiber layer number and orientations and demonstrated their ability to clot plasma and suppress bacterial growth. We see a direct application for this material as a component of wound dressings, since medical grade dextran is already commercially available and FDA-approved for medical applications. However, in the future, it could also be possible to use blends of other cross-linkable polymers with dextran to generate similar fabrics. Further studies employing circular dichroism spectroscopy or other analytical methods will be required to identify any interactions that might be present between incorporated drugs and the polymers used to form the fibers. These multicomponent fabric blends could potentially be used in more demanding applications for sustained drug delivery or as constructs for promoting wound healing.

5. Experimental Section

Dextran Formulations: Technical grade dextran (MW ≈500 000 g mol^{-1}; Pharmacosmos, Denmark) was dissolved at varying concentrations (10, 20, 30, 40, 50, 60, 70, 80, and 90 wt% in ddH_20 at room temperature on a rotary shaker for 24 h. The colloidal dextran solutions were then centrifuged to remove any air bubbles that were present in solution. Where applicable, the antibiotic (anti–anti from Life Technologies) or thrombin solutions (Equitech Bio, Kerrville, TX) were incorporated by gentle mixing with a pipette tip prior to fiber formation.

Fabric Formation: The viscous dextran solutions were applied at a volume of approximately ≈750 µL to wooden tongue depressors using a 1 cc syringe. The tongue depressors were then separated to elongate the dextran strings, which dried rapidly under ambient conditions. The strands of dextran solution (10–20 per elongation) were extended over a plastic cup containing metal weights to hold it in place. The fiber elongation procedure was repeated using the same tongue depressors, replenishing the dextran solution as needed to form fabrics of 50, 100, or 200 layers in three different orientations, unidirectional (180° symmetry), bidirectional (90° symmetry), or multidirectional (45° symmetry), by rotating the plastic cup between layers. The fabric specimens were cut from the cups and stored at room temperature or at –80 °C until later use.

Mechanical Testing: The fabrics specimens were cut into testing strips measuring ≈5 cm in length, 1 cm in width, with varying thicknesses for the 200, 100, and 50 layer fabrics. For each fabric thickness and fiber orientation, the test strips were cut in the directions horizontal, vertical, and diagonal to the primary direction of the fibers. The test strips were mounted on a Test Sources Model 1000 material testing machine for tensile testing using a 10 lb load cell. The test strips were placed within the grip calipers such that the total length between the calipers was 3.8 cm and pulled until failure at a displacement rate of 0.25 mm s^{-1}. The force–displacement data and stress–strain data were plotted in Sigmaplot with Sigmastat and the ultimate tensile strength was determined from the peak of the stress–strain curve.

Scanning Electron Microscopy: The fabrics were cut into 1 cm × 1 cm and mounted on SEM studs using conductive tape. The fabrics were imaged on FEI Quanta 3D SEM/FIB and Philips XL30ESEM systems using an accelerating voltage of 70 kV for the FEI SEM and 30 kV for the Philips ESEM at a pressure of 0.4 torr. The samples were imaged in their native state without metal coating.

Fibrin Clotting Assay: Fibrin clotting assays were carried out according to a previously published procedure with slight modifications.[42] Platelet-poor human plasma (purchased from Bioreclamation, Hicksville, NY) was thawed and centrifuged at 16.1 rcf for 5 min and then stored on ice while the microplate was prepared. Fabric punches were made with a 6 mm biopsy punch and weighed before they were used for plasma coagulation. The punches were stacked and cut as necessary to control the concentration of thrombin being delivered during the assay. This weight was 0.31 mg for most trials. The fabrics were then loaded in the microplate wells. Controls, such as the thrombin and no fabric conditions, were added to additional wells. A volume of 100 µL of plasma was then added simultaneously to each of the wells using a multichannel micropipette. The microplate was gently tapped for 5 s to promote mixing before starting the microplate reader, which was preconfigured to measure the light absorbance of the samples over time. The absorbance values were normalized according to

$$z_i = \frac{x_i - \min_x}{\max_x - \min_x}$$

where z_i is the normalized absorbance at 405 nm, x_i is the sample absorbance value at 405 nm, and $\max_x$ and $\min_x$ are the maximum and minimum absorbance values over the course of the assay, respectively. The maximum absorbance value typically occurred at the last time point (900s) of the test with thrombin and the lowest absorbance value was typically observed at the earliest time point (0s) of the test with thrombin.

Optical Microscopy: Clot formation was further examined using an Olympus BX51 microscope equipped with a light source and a linear polarizer. Ten microliters of plasma was placed on a glass coverslip. The fabric samples containing thrombin, the fabric alone, distilled water (1 µL) or thrombin alone were then added to the plasma. The final thrombin concentration was 31 U mL^{-1} for comparison with the clotting assay described above. After a 2 min incubation to allow coagulation, the samples were sandwiched between a second glass coverslip for brightfield imaging.

Agar Plate Assay: LB agar plates were prepared for a disk diffusion assay using BL21 *E. coli* cells. The *E. coli* cells were seeded on the LB agar plates and incubated at 37 °C for 1 h. The fabrics were made in the same fashion as those containing thrombin, except the antibiotic solution was used in place of thrombin. Dextran fabrics containing anti–anti were made using solutions of 50×, 5×, and 1× strength anti–anti in 50% dextran from an initial anti–anti solution of 10 000 U mL^{-1} penicillin, 10 000 mg mL^{-1} streptomycin, and 25 µg mL^{-1} fungizone (100× concentration). Fabrics with no antibiotics were used as controls. The plates were then removed from incubation and 6 mm diameter punches of the fabrics containing the various anti–anti concentrations were placed on the plates. The plates were incubated for an additional 24 h and photographed.

Supporting Information

Supporting Information is available from the Wiley Online Library or from the author.

Acknowledgements

The authors thank the Coulter Foundation Grant at University of Michigan for funding.

Received: May 23, 2014
Revised: August 14, 2014
Published online: September 10, 2014

[1] J. S. Boateng, K. H. Matthews, H. N. Stevens, G. M. Eccleston, *J. Pharm. Sci.* **2008**, *97*, 2892.
[2] D. J. Cole, R. J. Connolly, M. W. Chan, S. D. Schwaitzberg, T. K. Byrne, D. B. Adams, P. L. Baron, P. H. O'Brien, J. S. Metcalf, M. Demcheva, J. Vournakis, *Surgery* **1999**, *126*, 510.
[3] D. S. Katti, K. W. Robinson, F. K. Ko, C. T. Laurencin, *J. Biomed. Mater. Res. Part B: Appl. Biomater.* **2004**, *70*, 286.
[4] A. J. Meinel, O. Germershaus, T. Luhmann, H. P. Merkle, L. Meinel, European journal of pharmaceutics and biopharmaceutics : official journal of Arbeitsgemeinschaft fur Pharmazeutische Verfahrenstechnik e.V **2012**, *81*, 1.
[5] W. R. Wagner, J. M. Pachence, J. Ristich, P. C. Johnson, *J. Surg. Res.* **1996**, *66*, 100.
[6] T. J. Sill, H. A. von Recum, *Biomaterials* **2008**, *29*, 1989.
[7] A. R. Unnithan, N. A. Barakat, P. B. Pichiah, G. Gnanasekaran, R. Nirmala, Y. S. Cha, C. H. Jung, M. El-Newehy, H. Y. Kim, *Carbohydr. Polym.* **2012**, *90*, 1786.
[8] J. M. Yang, H. T. Lin, *J. Membr. Sci.* **2004**, *243*, 1.
[9] A. E. Pusateri, J. B. Holcomb, B. S. Kheirabadi, H. B. Alam, C. E. Wade, K. L. Ryan, *J. Trauma-Injury Infect. Crit. Care* **2006**, *60*, 674.
[10] M. W. Chan, S. D. Schwaitzberg, M. Demcheva, J. Vournakis, S. Finkielsztein, R. J. Connolly, *J. Trauma-Injury Infect. Crit. Care* **2000**, *48*, 454.
[11] R. Jayakumar, M. Prabaharan, P. T. Sudheesh Kumar, S. V. Nair, H. Tamura, *Biotechnol. Adv.* **2011**, *29*, 322.
[12] H. B. Kram, R. C. Nathan, F. J. Stafford, A. W. Fleming, W. C. Shoemaker, *Arch. Surg.-Chicago* **1989**, *124*, 385.
[13] B. Sorensen, O. H. Larsen, C. J. Rea, M. Tang, J. H. Foley, C. Fenger-Eriksen, *Semin. Thromb. Hemost.* **2012**, *38*, 268.
[14] F. H. Silver, M. C. Wang, G. D. Pins, *Biomaterials* **1995**, *16*, 891.
[15] X. H. Wang, Y. N. Yan, R. J. Zhang, *J. Bioact. Compat. Polym.* **2006**, *21*, 39.
[16] Z. M. Huang, Y. Z. Zhang, M. Kotaki, S. Ramakrishna, *Compos. Sci. Technol.* **2003**, *63*, 2223.
[17] C. Wenguo, Z. Yue, C. Jiang, *Sci. Technol. Adv. Mater.* **2010**, *11*, 014108.
[18] X. Jia, C. Zhao, P. Li, H. Zhang, Y. Huang, H. Li, J. Fan, W. Feng, X. Yuan, Y. Fan, *J. Biomater. Sci., Polym. Edn.* **2011**, *22*, 1811.
[19] H. Pan, H. Jiang, W. Chen, *Biomaterials* **2006**, *27*, 3209.
[20] H. Pan, H. Jiang, W. Chen, *Biomaterials* **2008**, *29*, 1583.
[21] H. Yoshimoto, Y. M. Shin, H. Terai, J. P. Vacanti, *Biomaterials* **2003**, *24*, 2077.
[22] F. Ignatious, L. H. Sun, C. P. Lee, J. Baldoni, *Pharm. Res.* **2010**, *27*, 576.
[23] H. Fong, I. Chun, D. H. Reneker, *Polymer* **1999**, *40*, 4585.
[24] M. Bognitzki, W. Czado, T. Frese, A. Schaper, M. Hellwig, M. Steinhart, A. Greiner, J. H. Wendorff, *Adv. Mater.* **2001**, *13*, 70.
[25] J. Doshi, D. H. Reneker, *J. Electrostat.* **1995**, *35*, 151.
[26] X. H. Zong, K. Kim, D. F. Fang, S. F. Ran, B. S. Hsiao, B. Chu, *Polymer* **2002**, *43*, 4403.
[27] M. Kacurakova, M. Mathlouthi, *Carbohydr. Res.* **1995**, *284*, 145.
[28] R. J. H. Stenekesa, H. Talsma, W. E. Hennink, *Biomaterials* **2001**, *22*, 1891.
[29] M. P. Bajgai, S. Aryal, S. R. Bhattarai, K. C. R. Bahadur, K.-W. Kim, H. Y. Kim, *J. Appl. Polym. Sci.* **2008**, *108*, 1447.
[30] H. Jiang, D. Fang, B. S. Hsiao, B. Chu, W. Chen, *Biomacromolecules* **2004**, *5*, 326.
[31] W. Ritcharoen, Y. Thaiying, Y. Saejeng, I. Jangchud, R. Rangkupan, C. Meechaisue, P. Supaphol, *Cellulose* **2008**, *15*, 435.
[32] G. L. Bowlin, D. G. Simpson, J. R. Bowman, S. W. Rothwell, US Patent CA 2721162 A1, **2009**.
[33] A. Ziabicki, *Fundamentals of Fibre Formation: the Science of Fibre Spinning and Drawing*, Wiley, London, New York **1976**.
[34] Y. Ohzawa, Y. Nagano, *J. Appl. Polym. Sci.* **1970**, *14*, 1879.
[35] Y. Ohzawa, Y. Nagano, T. Matsuo, *J. Appl. Polym. Sci.* **1969**, *13*, 257.
[36] S. H. Lee, Y. Kim, Y. Kim, *Carbohydr. Polym.* **2007**, *70*, 53.
[37] W. E. Teo, S. Ramakrishna, *Nanotechnology* **2006**, *17*, R89.
[38] J. K. Aronson, M. N. G. Dukes, *Meyler's Side Effects of Drugs : the International Encyclopedia of Adverse Drug Reactions and Interactions*, Elsevier, Amsterdam, Boston **2006**.
[39] W. L. Bloom, N. O. Fowler, J. A. Ward, R. H. Franch, *J. Surg. Res.* **1963**, *3*, 152.
[40] S. T. Hiippala, *Blood Coagul. Fibrin* **1995**, *6*, 743.
[41] P. Van der Linden, B. E. Ickx, *Can. J. Anaesth.-J. Can. D Anesth.* **2006**, *53*, S30.
[42] D. Tilley, I. Levit, J. A. Samis, *J. Vis. Exp.: JoVE* **2012**, 67, e3822.

